Neptunium and Manganese Biocycling in Nuclear Legacy Sediment Systems

Clare L. Thorpe[1], Katherine Morris[1], Jonathan R. Lloyd[1], Melissa A. Denecke[2], Kathleen A. Law[2], Kathy Dardenne[3], Christopher Boothman[1], Pieter Bots[1], Gareth T. W. Law[2*]

[1] Research Centre for Radwaste Disposal and Williamson Research Centre for Molecular Environmental Science, School of Earth, Atmospheric and Environmental Sciences, The University of Manchester, Manchester, M13 9PL, U.K.

[2] Centre for Radiochemistry Research, School of Chemistry, The University of Manchester, M13 9PL, U.K.

[3] Karlsruhe Institute of Technology, Institut Fur Nukleare Entsorgung, D-76021 – Karlsruhe, Germany.

*Corresponding author: Email: gareth.law@manchester.ac.uk; Tel: +44 (0)161 275 1428

Abstract

Understanding the behaviour of highly radiotoxic, long half-life radionuclide neptunium in the environment is important for the management of radioactively contaminated land and the safe disposal of radioactive wastes. Recent studies have identified that microbial reduction can reduce the mobility of neptunium *via* reduction of soluble Np(V) to the poorly soluble Np(IV), with coupling to both Mn(IV)- and Fe(III)- reduction implicated in neptunyl reduction. To further explore these processes Mn(IV) as δMnO_2 was added to sediment microcosms to create a sediment microcosm experiment "poised" under Mn(IV)-reducing conditions. Enhanced removal of Np(V) from solution occurred during Mn(IV)-reduction, and parallel X-ray absorption spectroscopy (XAS) studies confirmed Np(V) reduction to Np(IV) during Mn(IV)-reduction. Molecular ecology analysis of the XAS systems, which contained up to 0.2 mM Np showed no significant impact of elevated Np concentrations on the microbial population. These results demonstrate the importance of Mn cycling on Np biogeochemistry, and clearly highlight new pathways to reductive immobilisation for this highly radiotoxic element.

Introduction

Internationally, deep geological disposal is being considered as the long-term management and disposal option for higher activity radioactive wastes (HAW). A fundamental knowledge of reactions between radionuclides and geomedia is essential to underpin the safety case for geodisposal. Neptunium is a key risk-driving radionuclide in HAW due to its long half life (^{237}Np t½ = 2.1 x 10^6 years), ingrowth from ^{241}Am, high radiotoxicity, and relatively high solubility as Np(V). Indeed, Np is potentially the most mobile transuranic species in environments pertinant to deep geological disposal (e.g. Choppin and Stout, 1989; Kaszuba and Runde, 1999; Lloyd et al., 2000; Choppin, 2007; Law et al., 2010); further, Np is a persistant contaminant at or near nuclear sites (e.g., Cantrell, 2009; Morris et al., 2000; Stamper et al., 2013).

Neptunium is redox active and its environmental mobility can be affected by the biogeochmistry and redox conditions in the subsurface (Kaszuba and Runde, 1999; Lloyd et al., 2002; Choppin, 2007; Law et al., 2010). Under oxidising conditions Np is stable in solution as the soluble neptunyl cation, NpO_2^+, whilst under anaerobic conditions Np can be reduced to poorly soluble Np(IV) species (Kaszuba and Runde, 1999; Moyes et al., 2002; Llorens et al., 2005; Law et al., 2010; Bach et al., 2014). In the subsurface, microbial respiration can induce anaerobic conditions under which metals and radionuclides can be reduced (Lloyd and Renshaw, 2005). The development of bioreducing conditions is increasingly recognised as likely to be significant in the deep subsurface around a geological disposal facility (Pedersen, 2000; Fredrickson and Balkwill, 2006; Rizoulis et al., 2012; Williamson et al., 2013; Behrends et al., 2012), and is the basis for remediation of contaminated land where problematic radionuclides (e.g. Tc and U) may be reduced either enzymatically or indirectly *via* interactions with reduced species (e.g. Fe(II): Lloyd et al., 2002; Lloyd, 2003; Gadd, 2010; Newsome et al., 2014).

The ability of microorganisms to enzymatically reduce Np(V) to Np(IV) has been demonstrated in pure culture experiments (Lloyd et al., 2000; Icopini et al., 2007) although some microorganisms are unable to facilitate enzymatic Np(V) reduction (Songkasiri et al., 2002; Renshaw et al., 2005). Toxicity effects on selected metal-reducing bacteria are also of interest as studies with indigenous microorganisms highlight the tolerence of microorganisms to mM concentrations of Np (Law et al., 2010; Ams et al., 2013), whilst in pure culture experiments no toxicity effects were observed at Np concentrations less than 2mM (Ruggiero et al., 2005). In sediment systems, reductive immobilisation of Np(V) to Np(IV) has been observed during development of sediment anoxia with microbial metal reduction implicated in the reaction and with indirect (abiotic) reduction by Fe(II) shown to be possible (Law et al 2010).

Manganese is ubiquitous in soils and rock forming minerals and therefore, although Np interactions with Mn(IV) minerals have been studied previously (Wilk et al., 2005), a deeper understanding of Np(V) behaviour during early metal reduction (Mn(IV)- and Fe(III)-reduction) is essential in understanding its environmental behaviour in both deep and shallow subsurface environments. In addition, the potential importance of Mn in environmental actinide chemistry is increasingly recognised with Mn linked to both Pu and U cycling (Powell et al., 2006; Hu et al., 2010; Wang et al., 2013; Wang et al., 2014). Here we examine the behaviour of Np in sediment systems amended with labile Mn(IV) (δMnO_2) to allow microcosms to develop a period of extended or "poised" Mn reduction (Lovley and Philips, 1988). As well conducting experiments at low Np concentrations, we also collected XAS data from parallel experiments run at higher concentrations of Np. This allowed assessment of Np speciation and local-coordination under defined biogeochemical conditions. Finally, 16S rRNA gene analysis was performed to assess the response of the indigenous microbial communities to elevated Np concentrations.

Experimental Section

Safety

Neptunium (^{237}Np) is a high radiotoxicity alpha-emitting radionuclide with beta/gamma emitting progeny. Work can only be conducted by trained personnel in a certified, properly equipped radiochemistry laboratory, following appropriate risk assessment. The possession and use of radioactive materials is subject to statutory control.

Sample Collection

Sediments were collected from an area located ~ 2 km from the Sellafield reprocessing site in Calder River Valley, Cumbria during September 2012 (Lat 54°26'30 N, Long 03°28'09 W). Sediments were representative of the Quaternary unconsolidated alluvial flood-plain deposits that underlie the Sellafield site (Law et al., 2010) and were collected in sterile containers, sealed, and stored at 4 ºC prior to use (< 1 month).

Bioreduction Microcosms with Low NpO_2^+ concentrations

Sediment microcosms (10 ± 0.1 g Sellafield sediment, 100 ± 1 ml groundwater; in triplicate) were prepared using a synthetic groundwater representative of the Sellafield region (Wilkins et al., 2007) but with added nitrate and manganese (2 mM $NaNO_3$, 2 mM δMnO_2) and with 0.17 mmols of bioavailable Fe(III) in the sediment. Sodium acetate was also added in stoichiometric excess (10 mM) as an electron donor, the groundwater was sterilised (autoclaved for 1 hour at 120 ºC), purged with filtered 80 % / 20 % N_2 / CO_2, and pH adjusted to pH 7 (*via* drop-wise addition of 0.5 M HCl or 1M NaOH). Sediments and sterile groundwater were then added to sterile 120 ml glass serum bottles (Wheaton Scientific, USA) and sealed with butyl rubber stoppers using aseptic technique. Neptunium, as $^{237}NpO_2^+$

(20 Bq ml^{-1}; 3.2 μM; oxidation state verified by UV-Vis analysis) was then spiked into each microcosm; thereafter, the microcosms were incubated anaerobically at 21 ºC in the dark for 38 days. Throughout the incubation, sediment slurry was periodically extracted using aseptic technique, under an O_2-free, Ar atmosphere. The sediment slurry was centrifuged (15,000 g; 10 minutes) to separate sediment and porewater samples and ~ 0.5 g of sediment was stored at - 80 ºC for microbiological characterisation.

Geochemical Analyses

During microcosm sampling, total dissolved NO_2^-, Mn, and Fe concentrations were measured with standard UV-vis spectroscopy methods on a Jenway 6715 spectrophotometer (Lovley and Philips, 1987; Goto et al., 1997; Viollier et al., 2000; Harris and Mortimer, 2002). Aqueous NO_3^-, SO_4^{2-}, ammonium and acetate were measured by ion chromatography (Dionex ICS5000). Total bioavailable Fe(III) and the proportion of extractable Fe(II) in the sediment was estimated by digestion of 0.1 g of sediment in 5 ml of 0.5 N HCl for 60 minutes followed by the ferrozine assay, with and without added hydroxylammonium chloride (Lovley and Phillips, 1987; Viollier et al., 2000). The pH and Eh were measured with an Orion 420A digital meter and calibrated electrodes. Standards were routinely used to check the reliability of all methods and typically, calibration regressions had $R^2 \geq 0.99$. The elemental composition and bulk mineralogy of the sediment were determined by XRF (Thermo ARL 9400) and XRD (Philips PW 1050). Total organic carbon and total inorganic carbon were determined on a LECO CR-412 Carbon Analyser. The total ^{237}Np concentration in solution was measured by ICP- MS (Agilent 7500cx) using ^{232}Th as the internal standard.

XAS Experiments

Experiments were prepared to allow direct determination of Np speciation and local coordination environment in sediments under different geochemical conditions using X-ray Absorption Spectroscopy (XAS). Here, the elevated concentration of Np required for direct spectroscopic characterisation (0.2 mM Np(V) as NpO_2^+ in 0.07 M HCl) was added to microcosms containing 1g of sediment and 10 ml of groundwater that were poised at oxic, nitrate-, Mn-, Fe(III)-, and sulfate-reducing conditions, respectively. After Np(V) addition, the microcosms were left to incubate for 1 week in the dark at 7 ºC prior to geochemical sampling and subsequent freezing at – 80 ºC. Two additional Mn-reducing systems were also established where sediments had been enhanced with the addition of 2 mM δMnO_2: (i) 0.2 mM NpO_2^+ was added to an oxic microcosm that was then left to progress to Mn-reducing conditions (verified by the presence of Mn in porewaters and the absence of detectable 0.5 N extractable Fe(II) in sediments) before freezing at -80 ºC, and (ii) a parallel Mn-reducing microcosm (again with no detectable 0.5 N extractable Fe(II) in sediments) was sterilised by autoclaving (1 hour at 120 ºC) prior to the addition of 0.2 mM NpO_2^+, which was frozen at -80 ºC after 2 days of reaction. For XAS analysis, sediment samples were defrosted, centrifuged and ~ 0.5 g of sediment was packed (under anaerobic atmosphere if necessary) into airtight approved sample containers which were then triple contained and frozen until analysis. XAS analysis was conducted at the INE Beamline for Actinide Research at the ANKA synchrotron, Karlsruhe, Germany. Neptunium L_{III}-edge spectra (17610 eV) were collected in fluorescence mode by a 5 element solid-state Ge detector. Parallel K-edge measurements from a Zr foil were recorded for energy calibration. XANES data were collected for all samples and EXAFS data were collected for selected samples. Background subtraction, data normalisation and fitting to EXAFS spectra were performed using the software packages Athena and Artemis. The XANES edge-jump was tied to unity. Modeling of the EXAFS data in k^3 range was completed between 3 and 9.5 $Å^{-1}$.

156

157 ***Microbial community analysis***

158 Samples from an oxic sediment, and a Mn-reducing sample were taken from both low Np
159 (20 Bq ml^{-1}; 3.2 μM) and high Np (1.3 kBq ml^{-1}; 0.2 mM) microcosms and analysis
160 performed using PCR-based 16S rRNA gene analysis.

161

162 ***Ribosomal Intergenic Spacer Analysis***

163 DNA was extracted from Np containing microcosm samples (200 μl) using a PowerSoil
164 DNA Isolation Kit (MO BIO Laboratories INC, USA). The 16S-23S rRNA intergenic spacer
165 region from the bacterial RNA operon was amplified as described previously using primers
166 ITSF and ITSReub (Cardinale et al., 2004). The amplified products were separated by
167 electrophoresis in Tris-acetate-EDTA gel. The DNA was stained with ethidium bromide and
168 viewed under short-wave UV light. Positive microbial community changes identified by the
169 RISA justified further investigation by DNA sequencing of 16S rRNA gene clone libraries.

170 ***Amplification of 16S rRNA gene sequences***

171 A fragment of the 16S rRNA gene (approximately 1490 b.p.) was amplified from samples
172 using the broad-specificity primers 8F (Eden et al., 1991) and 1492R (Lane et al., 1985). PCR
173 reactions were performed in thin-walled tubes using a BioRad iCycler (BioRad, UK). Takara
174 Ex Taq Polymerase (Millipore, UK) was used to amplify DNA from the sample extract. The
175 PCR amplification protocol used with the 8F and 1492R primers was: initial denaturation at
176 94 ºC for 4 minutes, melting at 94 ºC for 30 seconds, annealing at 50 ºC for 30 seconds,
177 elongation at 72 ºC for 3 minutes and 35 cycles, followed by a final extension step at 72 ºC
178 for 5 minutes. The purity of the amplified products was determined by electrophoresis in tris-

acetate-EDTA (TAE) gel. DNA was stained with ethidium bromide and viewed under short-wave UV light using a BioRad Geldoc 2000 system (BioRad, UK).

Cloning

PCR products were purified using a QIAquick PCR purification kit (Qiagen, UK) and ligated directly into a cloning vector containing topoisomerase I-charged vector arms (Agilent Technologies, UK) prior to transformation into *E. coli* competent cells expressing Cre recombinase (Agilent Technologies, UK). White transformants that grew on LB agar containing ampicillin and X-Gal were screened for an insert using PCR. Primers were complementary to the flanking regions of the PCR insertion site of the cloning vector. The PCR method was: an initial denaturation at 94 ºC for 4 minutes, melting at 94 ºC for 30 seconds, annealing at 55 ºC for 30 seconds, extension at 72 ºC for 1 minutes and 35 cycles, followed by a final extension step at 72 ºC for 5 minutes. The resulting PCR products were purified using an ExoSap protocol, 2 µl of ExoSap mix (0.058 µl Exonuclease I, 0.5 µl Shrimp Alkaline Phosphatase and 1.442 µl H_2O) was added to 5 µl of PCR product and incubated at 37 ºC for 30 minutes followed by 80 ºC for 15 minutes.

DNA sequencing and phylogenetic analysis

Nucleotide sequences were determined by the dideoxynucleotide method. An ABI Prism BigDye Terminator Cycle Sequencing Kit was used in combination with an ABI Prism 877 Integrated Thermal Cycler and ABI Prism 377 DNA Sequencer (Perkin Elmer Applied Biosystems, UK). Sequences (typically 900 base pairs in length) were analysed using Mallard (Ashelford et al., 2006) to check for presence of chimeras or sequencing anomalies. Operational taxonomic units (OTU) were determined at a 98 % sequence similarity level using Mothur (Schloss et al., 2009). The individual OTU sequences were analysed using the

sequencing database of known 16S rRNA gene sequences provided on the Ribosomal Database Project (Cole et al., 2009) to identify nearest neighbours.

Results and discussion

Sediment characteristics

The sediment was dominated by quartz, feldspars (albite and microcline), and sheet silicates (muscovite and chlorite). The sediment had a high Si content (36.3 wt %) and contained Al (6.77 %), Fe (3.71 %), K (2.67 %), Na (0.92 %), Mg (0.75 %), Ti (0.38 %), Ca (0.27 %), and Mn (0.09 %). The total organic carbon content of the sediment was 0.69 % and total carbon was 1.70 %. The concentration of 0.5 N HCl extractable Fe in the sediment was 17.1 ± 1.6 mmol kg^{-1} prior to incubation and the sediment pH was ~ 5.

Neptunium behaviour during progressive bioreduction

Manganese enriched (2 mM δMnO_2) sediment microcosms amended with electron donor, and a Mn enriched sterile control microcosm, were spiked with 3.2 μM Np(V) (20 Bq ml^{-1}) and incubated over a 38 day period. Modelling of the initial groundwater chemistry in PHREEQC-2 (Specific Ionic Theory (SIT) database) predicted that the speciation of the Np in solution would be predominantly NpO_2^+ (see supporting information S1). In the sterile-control system, the pH remained stable and bulk biogeochemical changes indicative of terminal electron acceptor progression were not observed (Figure 1 A-F). A release of Mn (~0.2 mM) into the groundwater of the sterile control occurred when the sediments were autoclaved (Figure 1C) which is similar to past studies with this material (Thorpe et al., 2012). In the microbially-active Mn rich microcosms, terminal electron accepting processes progressed in the order NO_3^- > NO_2^- > Mn(IV) > Fe(III) > SO_4^{2-} reduction as expected (Figure 1B-E). In all microcosms, the pH remained circumneutral (Figure 1F), NO_3^-

decreased to < 0.2 mM within 11 days, and porewater Mn increased to between 0.05 – 0.1 mM after 9 days suggesting concomitant NO_3^- and Mn reduction in these systems (Figure 1C). Microbially-mediated Fe(III) reduction was then evident after 17 days as indicated by 0.5 N HCl extractable Fe(II) ingrowth to sediments. Importantly, in this system Mn reduction (indicated by Mn(II) in porewaters) occurred independently of any measurable Fe(III) reduction (indicated by a lack of Fe(II) ingrowth to sediments) across three time-points (days 7 to 11; Figure 1). The addition of 2 mM δMnO_2 to sediments resulted in an extended Mn-reducing 'period' which was distinguished from the Fe(III)-reduction in the microcosm so that Np-behaviour could be tracked throughout the stages of early metal reduction. In the sterile control the added Np(V) was partially sorbed to the sediment, with 22.0 % removed from solution after 7 days (Figure 1A). Thereafter, the concentration of Np in solution remained stable. Neptunyl sorption has been observed in to a similar extent in earlier studies using comparable sediment systems (Law et al., 2010) and has been attributed to sorption to negatively charged mineral surfaces (e.g. Fe(III)- or Mn(IV) -bearing minerals; Combes et al., 1992; Nakata et al., 2002; Arai et al., 2007; Müller et al., 2015; Wilk et al., 2005). In microbially active microcosms prior to the onset of Mn ingrowth to porewaters (0 - 7 days), 43.0 ± 1.9 % of the added Np was removed from the groundwater (Figure 1A). By day 11 where Mn(IV)-reducing conditions had developed, 86.0 ± 4.9 % of the added Np had been removed from solution. By the end of the experiment, following Fe(III) and subsequent SO_4^{2-} reduction at 38 days 96.1 ± 0.5 % of the added Np was removed to sediment. Enhanced removal of Np in active systems, compared to the sterile control, as observed in the first 7 days and prior to the onset of Mn reduction, could be attributed to either reduced surface reactivity in autoclaved sediments and / or enhanced Np(V) sorption to the system with microbial cells present (Gorman-Lewis et al., 2005; Ams et al., 2013). Results then show a clear relationship between Np(V) removal from solution and Mn reduction and

252 confirms that Np(V) is significantly removed from groundwater under Mn(IV)-reducing
253 conditions. It remains unclear in these low Np microcosm studies whether Np(V) removal is
254 linked to microbial metabolism or the result of abiotic reaction with Mn(II/III) minerals
255 produced during microbial Mn(IV) reduction. The formation of Np-carbonatohydroxo
256 complexes has been shown to increase the solubility of Np(IV) (Kitamura and Kohara, 2002;
257 Kim et al., 2010). However, in these systems under end point sulfate reducing conditions (pE
258 -4), and taking into account the increase in inorganic carbon expected from acetate utilization
259 (2 mM), solution modelling in PHREEQC-2 (SIT database) predicted that Np would be
260 speciated as $Np(OH)_4$ (see supporting information S2).
261
262 ***Neptunium L_{III}-edge XAS Experiments***
263 To assess the speciation of Np in sediment microcosms under different biogeochemical
264 conditions, select samples were run at the elevated concentrations required for XAS analysis:
265 oxic, nitrate-, Mn-, Fe(III)-, sulfate-, progressive Mn- and sterilized Mn- reducing. The
266 XANES of Np in the sterile, oxic control sediment and in the NO_3^- reducing sediment both
267 showed a Np(V)-like spectra displaying the characteristic multiple scattering resonance
268 structure at the high energy flank of the white line resulting from scattering along the axial
269 oxygen atoms of the linear neptunyl moiety (Figure 2; Moyes et al., 2002; Denecke et al.,
270 2005). Removal of Np from solution in both the oxic and nitrate reducing systems at
271 circumneutral pH is occurring and is likely due to Np(V) sorption to Fe or Mn mineral
272 surfaces (e.g. Combes et al., 1992; Nakata et al., 2002; Wilk et al., 2005; Arai et al., 2007;
273 Law et al., 2010; Müller et al., 2015). By contrast, the XANES spectra for the progressive
274 Mn-reducing microcosm, and the poised Mn(IV)-, Fe(III)-, and SO_4^{2-}- reducing systems
275 showed Np(IV)-like features with a loss of the multiple scattering resonance structure due to
276 the loss of the two neptunyl dioxygenyl oxygen backscatterers (Figure 2). Here, the enhanced

removal of Np from solution compared to the oxic or nitrate-reducing systems is attributed to reductive precipitation of Np(V) to Np(IV) (Law et al., 2010). In the absence of defined (matrix-matched) standards for these complex systems, linear combination fitting of the microbially-active Mn-reducing systems (both progressively reduced, and poised), using the oxic sediment and the sulfate-reducing sediment as end-members, indicated that Np(IV) was indeed the dominant oxidation state in both systems (>90 % Np(IV)) (Ravel et al., 2005). In contrast, the XANES spectra for the sterile Mn-reduced microcosm was Np(V) like (> 90 % Np(V)). Interestingly, the presence of significant Np(IV) (~90 %) in the microbially-active Mn(IV)-reducing systems and dominant Np(V) (~ 90 %) in the sterile Mn(IV)-reducing sediments suggests that microbial reduction of Np(V) to Np(IV) is significant in reductive immobilisation of Np(V). Any artefacts associated with mineral reactivity and reducing capacity of the sterile Mn(IV)-reducing sediment resulting from autoclaving cannot be ruled out here, but the significant change in Np(V) reduction between the microbially active and sterile sediments suggests enzymatic processes are likely to play a role in controlling Np(V) reductive immobilisation. These observations on sterile Mn(IV)-reducing sediments differ from those observed in a sterilised Fe(III)-reducing sediment reacted with Np(V), which facilitated Np(V) reduction (Law et al., 2010) and supports observations by Wilk et al. (2005) that observed reduction of Np(V) by Mn(II) bearing minerals (manganite and hausmannite) did not occur naturally but was instead caused by the high energy X-ray beam.

EXAFS data were also collected from the sterile oxic and microbially-active Mn-, and SO_4^{2-}-reducing samples. The k^3-weighted EXAFS spectra and their Fourier transform spectra are shown together with the corresponding best model fits (Figure 3; Table 1). The best fit to the sterilised oxic control sample was a Np(V)-like coordination environment with two axial oxygen backscatterers at 1.85 Å and four equatorial oxygen backscatterers at 2.51 Å (Table 1, Figure 3). The atomic distances for both axial and equatorial oxygen backscatterers are within

302 the range reported for Np(V) (1.82 – 1.88 Å; Combes et al., 1992; Moyes et al., 2002;
303 Denecke et al., 2005; Arai et al., 2007; Herberling et al., 2007; Law et al., 2010). The
304 statistical relevance of additional shells, containing Fe, Mn or Np, was assessed using an F-
305 test (Ravel et al., 2005) and it was found that no significant improvement to the model fit
306 could be achieved. The sulfate reducing sample was modelled using a Np(IV) like
307 coordination environment with eight oxygen backscatterers at a distance of 2.33 Å (Table 1,
308 Figure 3; Llorens et al., 2005; Law et al., 2010). In agreement with the linear combination
309 fitting, the best fit for the microbially active Mn(IV)-reducing sample was a Np(IV) like
310 coordination environment like the sulfate reducing system with eight oxygen backscatterers
311 at a distance of 2.31 Å. As with the oxic sediment sample, the addition of a second shell of
312 Fe, Np or Mn did not significantly improve the fit when using the F test as a measure of
313 validity. Finally it is noteworthy that in the samples where significant Np(IV) was present
314 and where EXAFS was possible (the Mn(IV)-reducing sediment and sulfate-reducing
315 microbially active sediments (Figure 3)), there was no evidence for a Np – O – Np interaction
316 of the type that would be expected for nano-particulate NpO_2, which has recently been
317 observed in environmentally relevant systems (Husar et al 2015). These observations are in
318 agreement with past work in sediment systems (Law et al 2010) which do not show
319 significant evidence for a Np – O – Np interaction.
320
321 ***Microbial community analysis***
322 Analysis of the microbial community in the Mn(IV)-reducing systems with low (3.2 μM) and
323 high (0.2 mM) Np content was performed to provide insight into the toxicity of Np(V) in
324 these systems. The biogeochemical trajectory was similar in sediments with both low and
325 high concentrations of Np suggesting that Np(V) was not significantly toxic to the microbial
326 community in these systems. These observations were supported by the RISA results, which

were similar across both low Np and high Np metal-reducing samples, and clone libraries for low and high Np samples, that confirmed broadly similar communities (Figure 4). Both high and low concentration Np experiments showed a decrease in biodiversity compared to the oxic sediment sample: clone libraries from the oxic sediment showed 34 operational taxonomic units (OTUs) from 71 clones whereas the biostimulated samples showed 7 OTUs from 92 clones in the low Np sample and 12 OTUs from 74 clones in the high Np sample. The clone libraries of both low and high Np concentration Mn-reducing samples were dominated (> 50 %) by members of the class *Bacillus,* including known denitrifying species consistent with the microcosms being primed with 2 mM nitrate prior to Mn reduction. The microorganisms responsible for Mn(IV) reduction could not be identified due to the complexity of the system.

Conclusions

Overall these data show that microbially-mediated Mn(IV)-reduction can lead to reductive immobilisation of Np(V) to Np(IV). The addition of bioavailable δMnO_2 provides a useful approach for prolonging microbial Mn(IV) reduction and allowing discrimination between the impacts of microbially-mediated Mn(IV) and Fe(III) reduction on radionuclide biogeochemistry. Removal of Np during Mn reduction was further maintained during Fe(III) and sulfate reduction and near complete removal of Np from solution had occurred by the onset of sulfate reduction. XANES data confirmed reduction to Np(IV) when Np was exposed to microbially active Mn(IV), Fe(III) and sulfate reducing sediments. Thermodynamically, Mn(IV) reduction is a more favourable process than Fe(III) reduction and so is likely to occur prior to Fe(III) reduction in subsurface environments where electron donor is limited. Although not conclusive these results imply that Np reduction in these systems occurs in the presence of active Mn-reducing cells rather than abiotically through

352 reaction with Mn(II) bearing minerals. Reduction of Np(V) by metal-reducing bacteria may
353 provide an additional mechanism for Np(V) removal from groundwater ahead of the
354 development of robust Fe(III)-reducing conditions. Results show the importance of
355 subsurface microbial manganese cycling on the speciation of neptunium. These data have
356 relevance to the fundamental understanding of Np behaviour in the shallow and deep
357 subsurface.
358

359 **Acknowledgments**

360 This work has been supported by the Natural Environmental Research Council grants
361 NE/H007768/1 and NE/L000547/1, an EPSRC University of Manchester / Sellafield Ltd.
362 KTA award for which we acknowledge Nick Atherton and the Sellafield Land Quality Team,
363 and STFC award ST/K001787/1. We thank Paul Lythgoe and Alastair Bewsher at The
364 University of Manchester, and Jörg Rothe (KIT-INE) for help with data
365 acquisition. Beamtime was obtained from the ANKA Lightsource (proposal number ANS-
366 85) with support from the EU Actinet Programme.
367

368 **References**

369 Ams, D.A., Swanson, J.S., Szymanowski, J.E.S., Fein, J.B., Richmann, M., Reed, D.T.
370 (2013). The effect of high ionic strength on neptunium(V) adsorption to a halophilic
371 bacterium. *Geochim. Cosmochim. Acta*, 110, 45-57.

372 Arai, Y., Moran, P. B., Honeyman, B.D., Davis, J.A. (2007). In situ spectroscopic evidence
373 for neptunium(V)-carbonate inner-sphere and outer-sphere ternary surface complexes
374 on hematite surfaces. *Environ. Sci. Technol.*, 41, 3940-3944.

375 Ashelford, K.E., Chuzhanova, N.A., Fry, J.C., Jones, A.J., Weightman, A.J. (2006). New
376 screening software shows that most recent large 16S rRNA gene clone libraries
377 contain chimeras. *Appl. Environ. Microbiol.,* 72, 5734–5741.

378 Bach, D., Christiansen, B.C., Schild, D., Geckeis, H. (2014). TEM study of green rust sodium
379 sulfate ($GRNa.SO_4$) interacted with neptunyl ions (NpO_2^+). *Radiochim. Acta,* 102(4),
380 279-290.

381 Behrends, T., Krawczyk-Bärsch, E., Arnold, T. (2012). Implementation of microbial processes
382 in the performance assessment of spent nuclear fuel repositories. *Appl. Geochem.,* 27,
383 453-462.

384 Cantrell, K.J. (2009). Transuranic contamination in sediment and groundwater at the U.S.
385 DOE Hanford site. US Department of Energy Report: PNNL-18640. Available at:
386 http://www.pnl.gov/main/publications/external/technical_reports/PNNL-18640.pdf

387 Cardinale, M., Brusetti, L., Quatrini, P., Borin, S., Puglia, A.M., Rizzi, A., Zanardini, E.,
388 Sorlini, C., Corselli, C., Daffonchio, D. (2004). Comparison of different primer sets
389 for use in automated ribosomal intergenic spacer analysis of complex bacterial
390 communities. *Appl. Environ. Microbiol.,* 70, 6147–6156.

391 Choppin, G.R., Stout, B.E. (1989). Actinide behaviour in natural waters. *Sci. Tot. Environ.,*
392 83, 203-216.

393 Choppin, G.R. (2007). Actinide speciation in the environment. *J. Radioanal. and Nucl.*
394 *Chem.,* 273, 695–703.

395 Cole, J.R., Wang, Q., Cardenas, E., Fish, J., Chai, B., Farris, R.J., Kulam-Syed-Mohideen,
396 A.S., McGarrell, D.M., Marsh, T., Garrity, G.M., Tiedje, J.M. (2009). The Ribosomal
397 Database Project: improved alignments and new tools for rRNA analysis. *Nucleic*
398 *Acids Res.*, 37, 141-145.

399 Combes, J.M., Chisholm-Brause, C.J., Brown, G.E., Parks, G.A., Conradson, S.D., Eller,
400 P.G., Triay, I.R., Hobart, D.E., Miejer, A. (1992). EXAFS spectroscopic study of
401 neptunium(V) sorption at the α-iron hydroxide oxide α-FeOOH/water interface.
402 *Environ. Sci. Technol.,* 26(2), 376-382.

403 Denecke, M.A., Dardenne, K., Marquardt, C.M. (2005). Np(IV)/Np(V) valence
404 determinations from Np L3-edge XANES/EXAFS. *Talanta*, *65*, 1008–1014.

405 Eden, P.E., Schmidt, T.M., Blakemore, R.P., Pace, N.R. (1991). Phylogenetic analysis of
406 *Aquaspirillum magnetotacticum* using polymerase chain reaction-amplified 16S
407 rRNA-specific DNA. *Int. J. Syst. Bacteriol.*, 41, 324-325.

408 Fredrickson, J.K., Balkwill, D.L. (2006). Geomicrobial processes and biodiversity in the deep
409 terrestrial subsurface. *Geomicro. J.*, 23, 345-356.

410 Gadd, G.M. (2010). Metals, minerals and microbes: geomicrobiology and bioremediation.
411 SGM prize lecture. *Microbiol.,* 156, 609-643.

412 Gorman-Lewis, D., Fein, J.B., Soderholm, L., Jensen, M.P., Chiang, M.H. (2005).
413 Experimental study of neptunyl adsorption onto Bacillus subtilis. *Geochim.*
414 *Cosmochim. Acta*, 69, 4837-4844.

415 Goto, K., Taguchi, S., Fukue, Y., Ohta, K., Watanabe, H. (1997). Spectrophotometric
416 determination of manganese with 1-(2-pyridylazo)-2-naphthol and a non-ionic
417 surfactant. *Talanta,* 24, 752-753.

418 Harris, S.J., Mortimer, R.J.G. (2002). Determination of nitrate in small water samples by the
419 cadmium-copper reduction method: A manual technique with application to the
420 interstitial waters of marine sediments. *Int. J. Environ. Anal. Chem.,* 82, 369- 376.

421 Herberling, F., Denecke, M.A., Bosbach, D. (2008). Neptunium(V) co-precipitation with
422 calcite. *Environ. Sci. Technol*. 42(2), 471-476.

423 Hu, Y., Schwaiger, L.K., Booth, C.H., Kukkadapu, R.K., Cristiano, E., Kaplan, D., Nitsche,
424 H. (2010) Molecular interactions of plutonium(VI) with synthetic manganese-
425 substituted goethite. *Radiochim. Acta,* 98, 655–663.

426 Husar, R., Hübner, R., Hennig, C., Martin, P.M., Chollet, M., Weiss, S., Stumpf, T., Zänker,
427 H., Ikeda-Ohno, A. (2015) Intrinsic formation of nanocrystalline neptunium dioxide
428 under neutral aqueous conditions relevant to deep geological repositories. *Chem.*
429 *Commun.*, 51, 1301-1304.

430 Icopini, G.A., Boukhalfa, H., Neu, M.P. (2007). Biological reduction of Np(V) and Np(V)
431 citrate by metal-reducing bacteria. *Environ. Sci. Technol*. 41(8), 2764-2769.

432 Kaszuba, J.P., Runde, W.H. (1999). The aqueous geochemistry of neptunium: Dynamic
433 control of soluble concentrations with applications to nuclear waste disposal. *Environ.*
434 *Sci. Technol.*, 33, 4427-4433.

435 Kim, B.Y., Oh, J.Y., Baik, M.H., Yun, J.I. (2010) Effect of carbonate on the solubility of
436 neptunium in natural granitic groundwater. Nuc. Eng. Technol., 42 (5), 552-561.

437 Kitamura, A., Kohara, Y., (2002) Solubility of neptunium(IV) in carbonate media. J. Nuc. Sci.
438 Technol., 3, 294-297.

439 Lane, D.J., Pace, B., Olsen, G.J., Stahl, D.A., Sogin, M.L., Pace, N.R. (1985). Rapid
440 determination of 16S ribosomal-RNA sequences for phylogenetic analysis. *P. Nat.*
441 *Acad. Sci. USA,* 82, 6955-6959.

442 Law, G. T. W., Geissler, A., Lloyd, J.R., Livens, F.R., Boothman, C., Begg, J.D.C., Denecke,
443 M.A., Rothe, J., Dardenne, K., Burke, I.T., Charnock, J.M., Morris, K. (2010).
444 Geomicrobiological redox cycling of the transuranic element neptunium. *Environ. Sci.*
445 *Technol.,* 44, 8924-8929.

446 Llorens, I., Den Auwer, C., Moisy, P., Ansoborlo, E., Vidaud, C., Funke, H. (2005).
447 Neptunium uptake by serum transferrin. *FEBS Journal,* 272, 1739-1744.

448 Lloyd, J.R., Yong, P., Macaskie, L.E. (2000). Biological reduction and removal of Np(V) by
449 two microorganisms. *Environ. Sci. Technol.,* 34, 1297-1301.

450 Lloyd, J.R., Chesnes, J., Glasauer, S., Bunker, D.J., Livens, F.R., Lovley, D.R. (2002).
451 Reduction of actinides and fission products by Fe(III)-reducing bacteria.
452 *Geomicrobiol. J.,* 19, 103-120.

453 Lloyd, J.R. (2003). Microbial reduction of metals and radionuclides. *FEMS Microbiol. Rev.*,
454 27, 411-425.

455 Lloyd, J.R., Renshaw, J.C. (2005). Bioremediation of radioactive waste: radionuclide-
456 microbe interactions in laboratory and field-scale studies. *Curr. Opin. Biotechnol.,* 16,
457 254-260.

458 Lovley, D. R., Phillips, E. J. P. (1988). Manganese inhibition of microbial iron reduction in
459 anaerobic sediments. *Geomicrobiol. J.,* 6, 145-155.

460 Lovley, D.R., Phillips, E.J.P. (1987). Rapid assay for microbially reducible ferric iron in
461 aquatic sediments. *Appl. Environ. Microbiol.*, 53, 1536-1540.

462 Morris, K., Butterworth, J.C., Livens, F.R. (2000). Evidence for the remobilization of
463 Sellafield waste radionuclides in an intertidal salt marsh, West Cumbria, UK. *Estuar.*
464 *Coast. Shelf S.*, 51, 613-625.

465 Moyes, L.N., Jones, M.J., Reed, W.A., Livens, F.R., Charnock, J.M., Mosselmans, J.F.W.,
466 Hennig, C., Vaughan, D.J., Pattrick, R.A.D. (2002). An X-ray absorption
467 spectroscopy study of neptunium(V) reactions with mackinawite (FeS). *Environ. Sci.*
468 *Technol.*, 36, 179-183.

469 Müller, K., Gröschel, A., Rossberg, A., Bok, F., Franzen, C., Brendler, V., Foerstendorf, H.
470 (2015). In situ spectroscopic identification of neptunium(V) inner-sphere complexes
471 on the hematite water interface. *Environ. Sci. Technol.*, 49, 2560-2567.
472 Nakata, K., Nagasaki, S., Tanaka, S., Sakamoto, Y., Tanaka, T., Ogawa, H. (2002). Sorption
473 and reduction of neptunium(V) on the surface of iron oxides. *Radiochim. Acta,* 90(9-
474 11), 665-669.
475 Newsome, L., Morris, K., Lloyd, J.R. (2014). The biogeochemistry and bioremediation of
476 uranium and other priority radionuclides. *Chem. Geo.,* 363, 164-184.
477 Pedersen, K. (2000). Exploration of deep intraterrestrial microbial life: current perspectives.
478 *FEMS Microbiol. Lett.,* 185, 9-16.

479 Powell, B.A., Duff, M.C., Kaplan, D.I., Field, R.A., Newville, M., Hunter, D.B., Bertsh, P.M.,
480 Coates, J.T., Eng, P., Rivers, M.L., Serkiz, S.M., Sutton, S.R., Triay, I.R., Vaniman,
481 D.T. (2006). Plutonium oxidation and subsequent reduction by Mn(IV) minerals in
482 Yucca Mountain tuff. *Environ. Sci. Technol.,* 140(11), 3508-3514.

483 Ravel, B., Newville, M. (2005). ATHENA, ARTEMIS, HEPHAESTUS: Data analysis for X-
484 Ray absorption spectroscopy using IFEFFIT. *J. Synchro. Rad.*, 12, 537−541.

485 Renshaw, J.C., Butchins, L.J.C., Livens, F.R., May, I., Charnock, J.M., Lloyd, J.R. (2005).
486 Bioreduction of uranium: Environmental implications of a pentavalent intermediate.
487 *Environ. Sci. Technol.*, 39, 5657-5660.

488 Rizoulis, A., Steele, H.M., Morris, K., Lloyd, J.R. (2012). The potential impact of microbial
489 metabolism during the geodisposal of intermediate level waste. *Mineral. Mag*., 76,
490 3261-3270.

491 Ruggiero, C.E., Boukhalfa, H., Forsythe, J.H., Lack, J.G., Hersman, L.E., Neu, M.P. (2005).
492 Actinide and metal toxicity to prospective bioremediation bacteria. *Environ.*
493 *Microbiol.*, 7, 88-97.

494 Stamper, A., McKinlay, C., Coughlin, D., Laws, F. (2013). Groundwater Annual Report
495 2012. Sellafield Ltd, Technical report: LQTD000032

496 Schloss, P.D., Westcott, S.L., Ryabin, T., Hall, J.R., Hartmann, M., Hollister, E.B.,
497 Lesniewski, R.A., Oakley, B.B., Parks, D.H., Robinson, C.J., Sahl, J.W., Stres, B.,
498 Thallinger, G.G., Van Horn, D.J., Weber, C.F. (2009). Introducing mothur: Open-
499 source, platform-independent, community-supported software for describing and
500 comparing microbial communities. *Appl. Environ. Microbiol.*, 75, 7537-7541.

501 Songkasiri, W., Reed, D.T., Rittmann, B.E. (2002). Bio-sorption of neptunium(V) by
502 *Pseudomonas fluorescens. Radiochim. Acta*, 90, 785-789.

503 Thorpe, C.L., Law, G.T.W., Boothman, C., Lloyd, J.R., Burke, I.T., Morris, K. (2012).
504 Synergistic effect of high nitrate concentrations on sediment bioreduction.
505 *Geomicrobiol. J.*, 29, 484-493.

506 Viollier, E., Inglett, P.W., Hunter, K., Roychoudhury, A.N., Van Cappellen, P. (2000). The
507 ferrozine method revisited: Fe(II)/Fe(III) determination in natural waters. *Appl.*
508 *Geochem.,*15, 785-790.

509 Wang, Z., Lee, S.W., Kapoor, P., Tebo, B.M. and Giammar, D.E. (2013). Uraninite oxidation
510 and dissolution induced by manganese oxide: A redox reaction between two insoluble
511 minerals. *Geochim. Cosmochim. Acta,* 100(1), 24-40.

512 Wang, Z., Xiong, W., Tebo, B.M. and Giammar, D.E. (2014). Oxidative UO_2 dissolution
513 induced by soluble Mn(III). *Environ. Sci. Technol.,* 48 (1), 289-298.

514 Wilk, P.A., Shaughnessy, D.A., Wilson, R.E., Nitsche, H. (2005). Interfacial interactions
515 between Np(V) and manganese oxide minerals manganite and hausmannite. *Environ.*
516 *Sci. Technol.,* 39, 2608-2615.
517 Wilkins, M.J., Livens, F.R., Vaughan, D.J., Beadle, I., Lloyd, J.R. (2007). The influence of
518 microbial redox cycling on radionuclide mobility in the subsurface at a low-level
519 radioactive waste storage site. *Geobiol.*, 5, 293-301.
520 Williamson, A.J., Morris, K., Shaw, S., Byrne, J.M., Boothman, C., Lloyd, J.R. (2013).
521 Microbial reduction of Fe(III) under alkaline conditions relevant to geological
522 disposal. *Appl. Environ. Microbiol*., 79(11), 3320-3326.
523

Figure Legends

Figure 1. Microcosm incubation time-series data (days 0-37). (A) Np in porewaters, (B) NO_3^- in porewaters, (C) Mn in porewaters, (D) 0.5 N HCl % extractable sedimentary Fe as Fe(II), (E) SO_4^{2-} in porewaters. ■ = microbially active microcosms; ● = sterile control microcosms. Initial pH in all microcosms was ~ 7. Error bars represent 1σ experimental uncertainty from triplicate microcosm experiments (where not visible error bars are within symbol size).

Figure 2. Np L_{III}–edge XANES spectra for Np amended sediments under different biological conditions. Spectra from oxic sediment, nitrate-reducing sediment and sterilised Mn-reducing sediment samples show the Np(V) like multiple scattering resonance structure resulting from high energy scattering along the axial oxygen atoms of the linear neptunyl moiety. Spectra from Mn-, Fe(III)-, sulfate- and progressive Mn-reducing sediment samples do not contain this feature and are therefore more typical of Np(IV) XANES.

Figure 3. EXAFS spectra and Fourier transforms (uncorrected for phase shift of backscattering atoms) for Np on sediments under different geochemical conditions. From top to bottom: oxic, Mn- and sulfate-reducing conditions. Black lines are k^3-weighted data and grey lines are the best model fits to the data.

Figure 4. Microbial community analysis of (A) Oxic sediment at 0 days; (B) Mn-reducing sediment amended with 3.2 μM ^{237}Np; (C) Mn reducing sediment amended with 0.2 mM ^{237}Np.

549 **Table 1**
550 EXAFS modelling of Np L_{III} edge spectra for Np associated with sediments under different
551 biogeochemical conditions.

	Path	Type	*CN*	*R* (Å)	σ^2 (Å^2)	X_v^2	*R*
Oxic	1 2	O O	2 4	1.86 2.45	0.006 0.021	59.8	0.0079
Mn Red	1	O	8	2.31	0.014	217.3	0.0130
Sul Red	1	O	8	2.34	0.012	98.9	0.0227

552 *CN* is the coordination number, R is the interatomic distance, σ^2 is the Debye-Waller factor
553 (Å^2), X_v^2 reduced chi square value and *R* is the least squares residual and is a measure of the
554 overall goodness of fit.
555

556

557

558

559

Figure 1

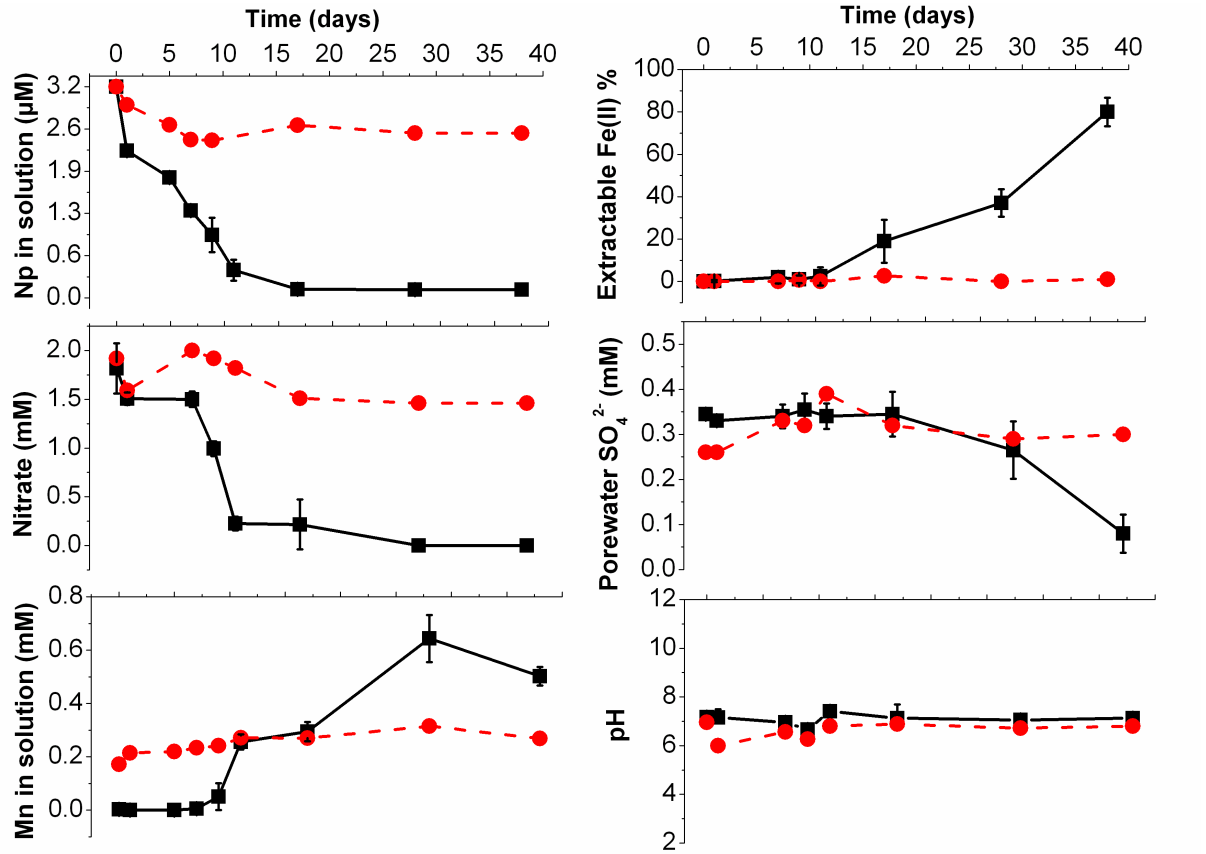
Time (days)
Np in solution (µM)
Nitrate (mM)
Mn in solution (mM)
Extractable Fe(II) %
Porewater SO_4^{2-} (mM)
pH

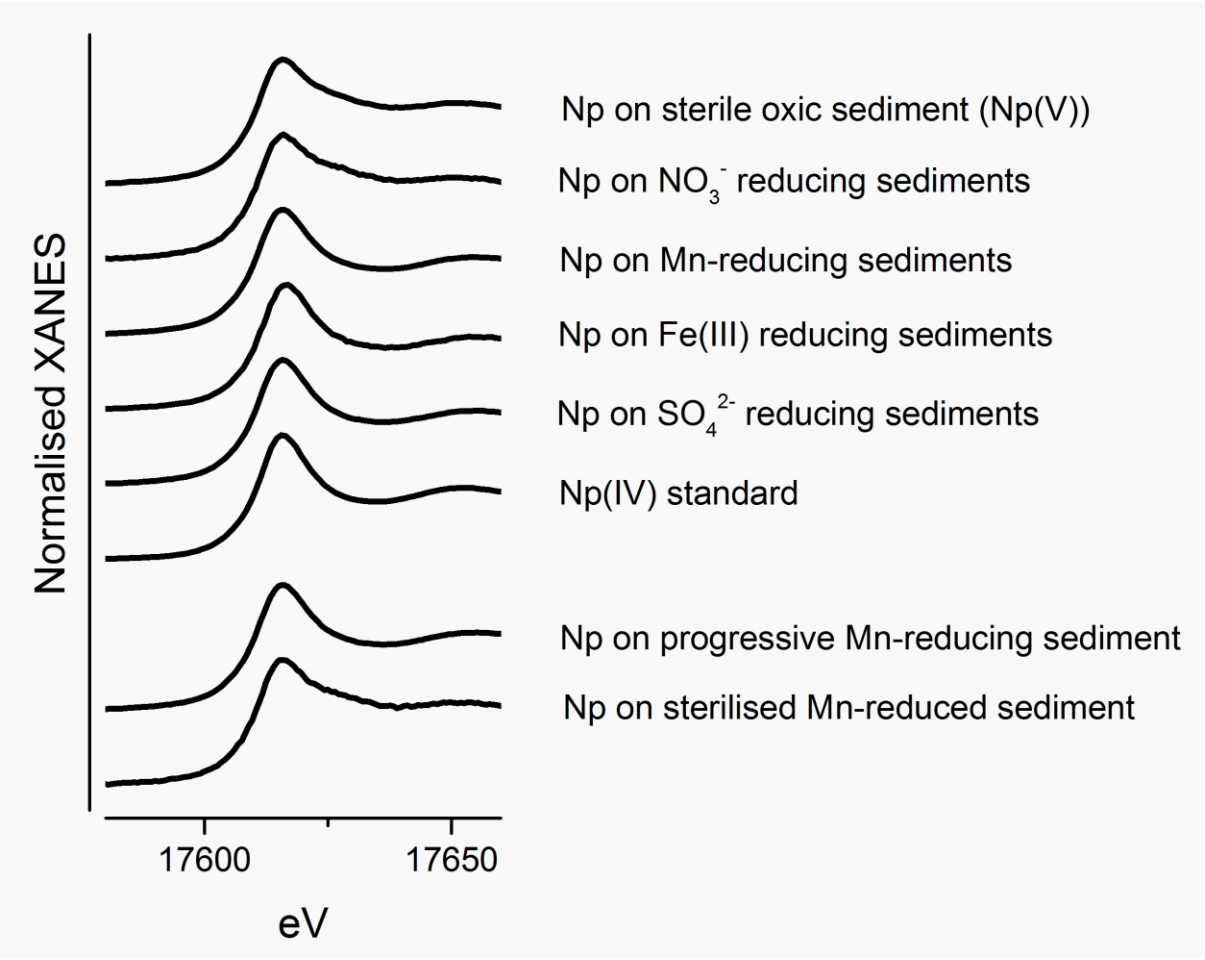

574

575 **Figure 2**

576

577

578

579

580

581

582

583

584

585

586

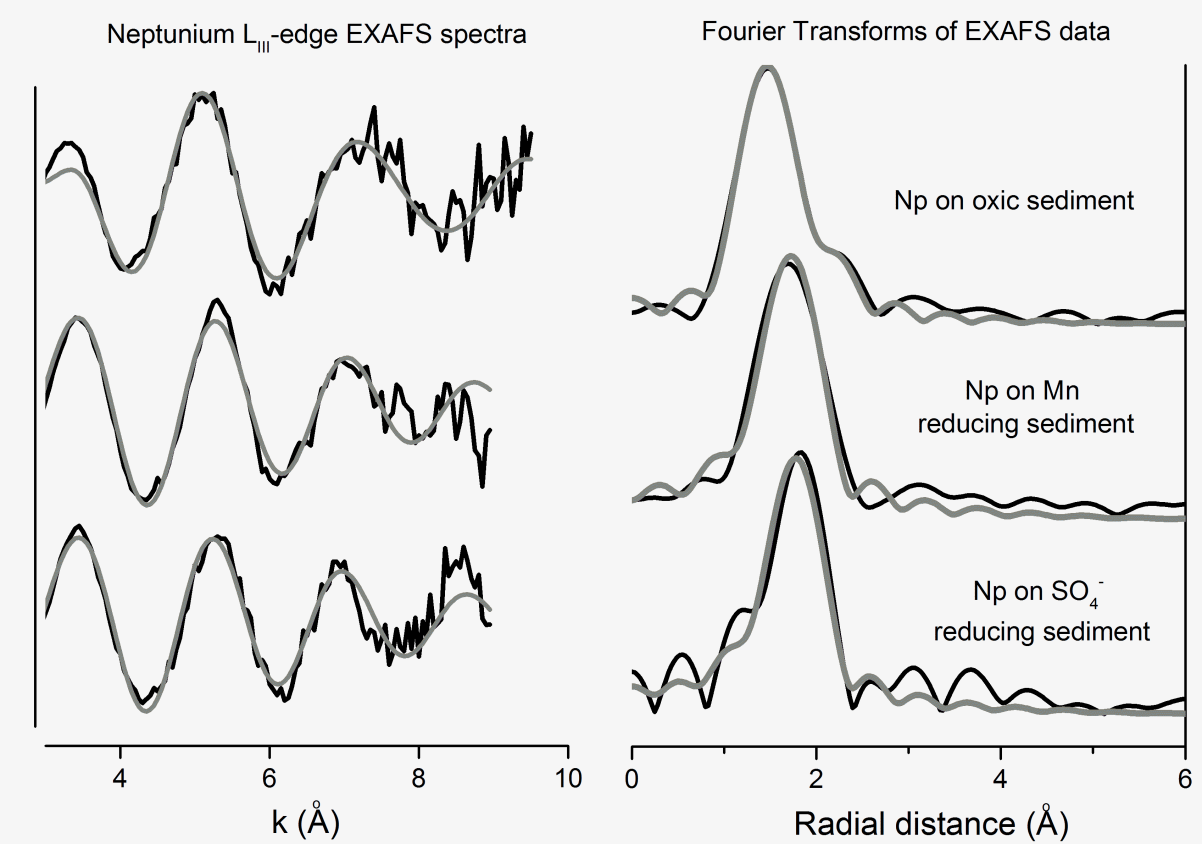
Neptunium L_{III}-edge EXAFS spectra
Fourier Transforms of EXAFS data
Np on oxic sediment
Np on Mn
reducing sediment
Np on SO_4^-
reducing sediment
4
6
8
10
k (Å)
0
2
4
6
Radial distance (Å)

Figure 3

Figure 4

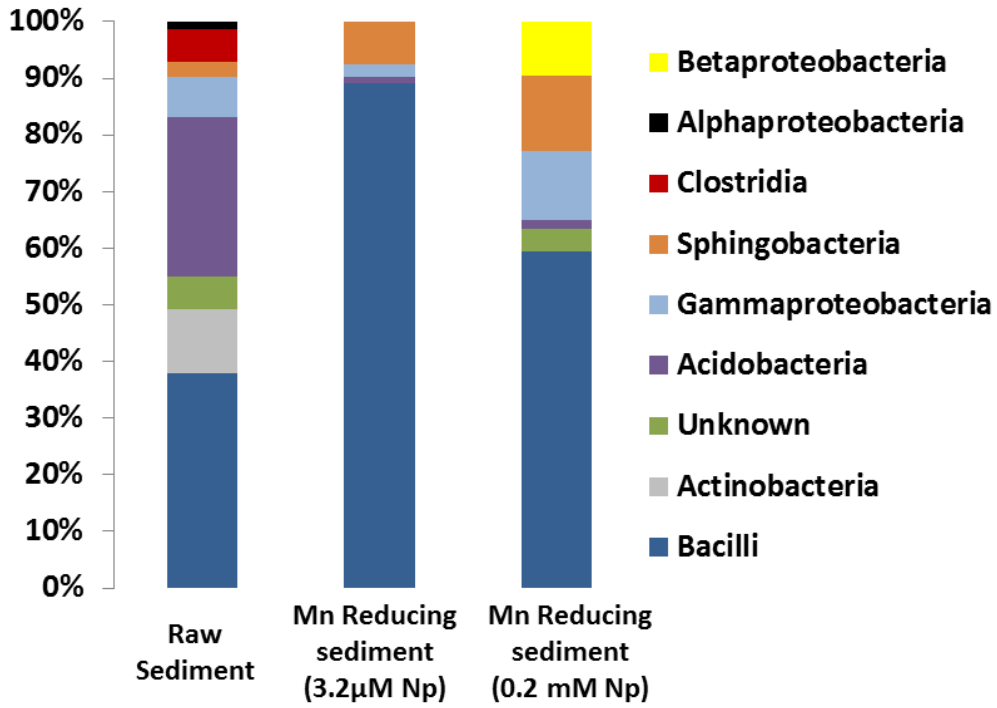
100%
90%
80%
70%
60%
50%
40%
30%
20%
10%
0%
Raw Sediment
Mn Reducing sediment (3.2µM Np)
Mn Reducing sediment (0.2 mM Np)
Betaproteobacteria
Alphaproteobacteria
Clostridia
Sphingobacteria
Gammaproteobacteria
Acidobacteria
Unknown
Actinobacteria
Bacilli